Generic Darwinian Selection in Catalytic Protocell Assemblies

Andreea Munteanu
Camille Stephen-Otto Attolini
Steen Rasmussen
Hans Ziock
Ricard V. Solé

SFI WORKING PAPER: 2006-09-032

SFI Working Papers contain accounts of scientific work of the author(s) and do not necessarily represent the views of the Santa Fe Institute. We accept papers intended for publication in peer-reviewed journals or proceedings volumes, but not papers that have already appeared in print. Except for papers by our external faculty, papers must be based on work done at SFI, inspired by an invited visit to or collaboration at SFI, or funded by an SFI grant.

©NOTICE: This working paper is included by permission of the contributing author(s) as a means to ensure timely distribution of the scholarly and technical work on a non-commercial basis. Copyright and all rights therein are maintained by the author(s). It is understood that all persons copying this information will adhere to the terms and constraints invoked by each author's copyright. These works may be reposted only with the explicit permission of the copyright holder.

www.santafe.edu

SANTA FE INSTITUTE

Generic Darwinian selection in catalytic protocell assemblies

Andreea Munteanu*

ICREA-Complex Systems Lab, Universitat Pompeu Fabra, Dr. Aiguader 80, 08003 Barcelona, Spain

Camille Stephan-Otto Attolini

Universität Wien, Währingerstraße 17, A-1090 Wien, Austria

Steen Rasmussen†

SOS, EES6 MS D-462 Los Alamos National Laboratory, Los Alamos, NM 87545, U.S.A. and Santa Fe Institute, Santa Fe, NM 87501, U.S.A.

Hans Ziock

SOS, EES6 MS D-462 Los Alamos National Laboratory, Los Alamos, NM 87545, U.S.A.

Ricard V. Solé

ICREA-Complex Systems Lab, Universitat Pompeu Fabra, Dr. Aiguader 80, 08003 Barcelona, Spain and Santa Fe Institute, Santa Fe, NM 87501, U.S.A.

To satisfy the minimal requirements for life, an information carrying molecular structure must be able to convert resources into building block and also be able to adapt to or modify its environment to enhance its own proliferation. Furthermore, new copies of itself must have variable fitness such that evolution is possible. In practical terms a minimal protocell should be characterised by a strong coupling between its metabolism and genetic subsystem which is made possible by the container. There is still no general agreement on how such a complex system might have been naturally selected for in a prebiotic environment. However, the historical details are not important for our investigations as they are related to assembling and evolution of protocells in the laboratory. Here we study three different, minimal protocell models of increasing complexity, all of them incorporating the coupling between a "genetic template", a container, and eventually a toy metabolism. We show that, for any local growth law associated with template self-replication, the overall temporal evolution of all protocell's components follows an exponential growth (efficient or uninhibited autocatalysis). Thus, such a system attains exponential growth through coordinated catalytic growth of its component subsystems, independent of the replication efficiency of the involved subsystems. As exponential growth implies the survival of the fittest in a competitive environment, these results suggest that protocell assemblies could be efficient vehicles in terms of evolving through Darwinian selection.

Keywords: protocell, replicator dynamics, catalytic coupling, prebiotic evolution

I. INTRODUCTION

Cells are the basic structural and functional units of all known life, performing the vital functions of an organism and containing the hereditary information necessary for self-regulation and self-replication. The complexity of modern cells and life itself is a consequence of open-ended evolution whose beginnings are associated with the origin of life on Earth. Even though many of the main issues associated to the emergence of life remain to be established, significant progress has been made since Oparin's original vision of the origin of life (Oparin 1957) and Gánti's model of a minimal cell (Gánti 1975).

These advances have steadily pushed the experimental implementation as well as the understanding of protocells ever closer to reality (Kaneko & Yomo 2000; Luisi et al. 2006; Monnard et al. 2002; Paul & Joyce 2004; Rasmussen et al. 2004; Segré et al. 2001; Stadler & Stadler 2003; Szostak et al. 2001; Takakura et al. 2003). For a protocell to function properly, it must contain both genes and a metabolism, which are integrated by a container. The interdependence and cross-regulation of these subsystems is a major issue. Regardless of which of the protocellular subsystems a work centres on, templates, energetics, or container, the concept of self-replication is central, be it an experimental scenario or a theoretical model.

One important problem is the overall kinetic behaviour of template replication. Information in biological systems is stored in, and is propagated by template molecules capable of making copies of themselves. Due to the product inhibition by the new complementary templates in a naked gene replication process, the kinetics has been shown to be parabolic (Bag & von Kiedrowski 1996), i.e. sub-exponential, and prevent Darwinian selection. Since

*Electronic address: andreea.munteanu@upf.edu
†Electronic address: steen@lanl.gov

exponential growth is known to be a key feature of Darwinian selection, where the fittest variants win over the less-fit ones, the lack of exponential growth for reproducers would be an obstacle to their success. In spite of our intuition, which might suggest that selection at the cellular level should become slower than parabolic when based on parabolic template dynamics, here we show quite the opposite: the selection process in catalytically coupled assemblies of protocells is Darwinian, with coordinated exponential growth of all involved components and thus survival of the fittest, independent of the template growth law. The present work investigates a class of minimal catalytically coupled protocell models and is centred on the relation between internal dynamics and the global population-level dynamics of protocells.

II. BASIC GROWTH DYNAMICS

From simple models of prebiotic evolution, a few basic growth laws resulted as being fundamental for replicators dynamics. These in turn have remarkable implications for the selection among competing processes (Eigen & Schuster 1979; Szathmáry 1991). The primary replication process, the fission of the progenitor, gives rise to exponential growth in the absence of ecological constraints (Malthusian growth). Here, the growth rate of the population is proportional to the population itself, *i.e.* $\dot{x} = kx$, where "$\cdot$"implies a time derivative. When two exponentially growing populations compete, the one with the greater growth rate completely excludes its competitor, a case referred to as "the survival of the fittest". Additionally, two other simple non-Malthusian processes are often considered in the literature: a faster and a slower growth, respectively, than the exponential one (Table I). While the former, generally referred to as hyperbolic growth ($\dot{x} = kx^p$, $p > 1$), is associated with models of mutualistic replicators (hypercycles: Eigen 1971), the latter (parabolic growth: $\dot{x} = kx^p$, $p < 1$) is typical for experimental template-directed replication ($p = 0.5$) (von Kiedrowski 1986). Note that constant growth is also possible in this framework ($p = 0$).

TABLE I Growth laws

Growth Law	$\dot{x} = kx^p$, $p > 0$
General Solution	$x(t) = \begin{cases} [x_0^{1-p} + (1-p)kt]^{1/(1-p)} & \text{for } p \neq 1 \\ x(t) = x_0\, e^{kt} & \text{for } p = 1 \end{cases}$
Particular Cases	$p = 0$: constant $p = 1/2$: pure parabolic $p = 1$: exponential $p = 2$: pure hyperbolic

One can notice that for two coexistent parabolically-growing populations[1], "the survival of everybody" is guaranteed, while for two hyperbolically[2] growing populations, the one with the highest initial concentration times the growth rate (*i.e.* $x_0 k$) will outgrow the other (Eigen & Schuster 1979; Szathmáry & Maynard-Smith 1997). While referred to as "the survival of the common" case, it is not guaranteed that the most common hyperbolically growing population will always invade when rare. Which one wins is determined by the ratio between initial populations (initial conditions), on one hand, and the fitness constants (reaction constants), on the other hand (consider the case $p = 2$ in Table I). Although Darwinian evolution, *i.e.* survival of the fittest, is possible for the hyperbolic case, the clearest example of Darwinian evolution is provided by exponential growth.

III. TEMPLATE DIRECTED REPLICATION

Among all systems with auto-catalytic synthesis of their constituent molecules, the most relevant to the origin of life is the one based on non-enzymatic template directed replication (Orgel 1992). In the last two decades, various experimental works have been dedicated to the in-depth study of such simple systems with emphasis on artificial "self-replication" (Robertson et al. 2000). Several research groups were able to experimentally demonstrate a sigmoidal time evolution of template concentration (Lee et al. 1996; von Kiedrowski et al. 1991). Such behaviour is a consequence of the exponential growth of the product (*i.e.* template) in the presence of a limited number of available building blocks (limited resources). Von Kiedrowski and coworkers were the first to obtain self-complementary artificial replication (von Kiedrowski 1986) and showed a growth order $p = 1/2$ (parabolic growth) instead of $p = 1$ (exponential growth) as expected from a true auto-catalytic replication. Parabolic growth has been proved to be the result of product inhibition which decreases the efficiency of the auto-catalytic cycle (Bag & von Kiedrowski 1996).

As described in the previous section, the auto-catalytic growth order is of great importance in establishing the long-term evolution of the system through selection processes. Interestingly enough, Rocheleau et al. (2006) proved that in spite of an internal parabolic growth of template concentration in a simple model of template-container coupling, the total template concentration considered over the entire population of protocells turns out to be exponential. More surprisingly, the catalytically coupled protocells containers follow an exponential

[1] Populations characterised by the same growing exponent.

[2] For the cases $1 - p < 0$, there exists a time value t_∞ at which the bracket term in the general solution from Table I becomes zero and due to the negative $(1 - p)$ exponent, $x(t_\infty)$ is infinite. Thus, the range of applicability is $0 \leq t \leq t_\infty$.

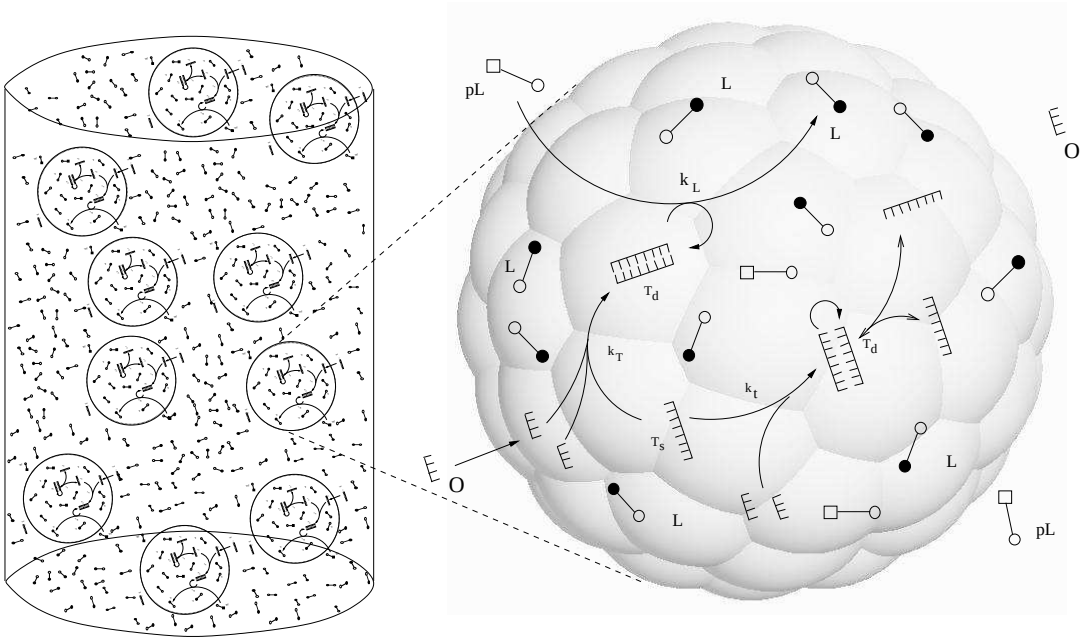

FIG. 1 A simple model of protocell replication involving template-catalysed formation of lipid molecules. This is the simplest scenario of coupled template-container organisation. The circular features representing the individual protocells consist of a micellar container built of lipid molecules (L) among which are embedded the templates (T: s=single-,d=double-stranded), the lipid precursors (pL) and the resource template oligomers (O). The "k's" are the rate constants.

growth with the same exponent as the templates' growth. This result is significant as a proof of regulated template-container interdependence, ensuring a correlated growth of the system's parts. This work thus demonstrates that a stoichiometric coupling between the protocell's subsystems is not compulsory, as suggested by others (Gánti 2003) and that cross-regulation of the subsystems occurs naturally as a consequence of catalysis. In the present work, we shall demonstrate that this result holds for any type of local growth dynamics of templates in the model of Rocheleau et al. (2006), as well as in extended and more realistic versions which include metabolic reaction steps.

IV. TEMPLATE-CONTAINER COUPLING

In Rocheleau et al. (2006), the template-container system was effectively defined by the chemical reactions

$$\alpha\, O + T_s \xrightarrow{k_T} T_d \tag{1a}$$

$$T_d \xleftrightarrow{K_t} 2Ts \tag{1b}$$

$$pL + T_d \xrightarrow{k_L} T_d + L\ , \tag{1c}$$

where T_s, T_d and L represent the single-strand template, the double-strand template and the lipid molecules, respectively, while O and pL are respectively the single-stranded template and lipid precursors whose concentrations are kept constant, with α denoting the necessary stoichiometry for the template directed replication. The graphical representation of the chemical reactions appears in Fig. 1. The hybridisation and the dehybridisation are considered in equilibrium [reaction (1b)] as long as the template replication [reaction (1a)] is a significantly slower process in comparison. The former condition leads to the equilibrium constant $K_t = [T_s]^2/[T_d]$, where the brackets denote concentration (molarity). As expected from experimental work, when dehybridisation is much slower than hybridisation (*i. e.* product inhibition), one has $K_t \ll 1$ since $[T_d] \gg [T_s]$.

Rocheleau et al. define the total single-strand concentration as $[T_l] \equiv 2[T_d] + [T_s]$ and consider that the protocells grow by intake of nutrients (*i.e.* precursors) and divide when a predefined critical size is reached. The existence of a critical size for micellar structures is supported by both experiments and theory (Bachman et al. 1992; Mavelli 2004), even if the growth-division process still lacks a complete experimental and theoretical proof. Additionally, the aggregates are envisioned as composed mainly of lipids, with the other molecules existing at very low concentrations diluted in the local lipid solution.

A. Constant Volume

By applying the standard chemical kinetics to the reactions (1a)-(1c), one finds that the local total template and lipid concentrations evolve according to

$$[\dot{T}_l] = C_T[T_l]^p \text{ with } p = 1/2 \quad (2a)$$
$$[\dot{L}] = C_L[T_l] \ , \quad (2b)$$

where $C_T \equiv k_T f([O])\sqrt{K_t/2}$ for $p = 1/2$, and $C_L \equiv k_L[pL]/2$ are constants [3] and "$\cdot$"implies a time derivative (see Appendix A). The term $f([O])$ is a function depending on oligomer stoichiometry (the number of oligomers) needed for each template replication. As we consider that the oligomers are present in abundance and thus the oligomer concentration can be approximated to constant, this function term is also a constant. Local refers to the concentration within the container itself. Considering a general case of eq. (2a), the local dynamics of the templates is parabolic if $p < 1$, exponential, if $p = 1$, and hyperbolic if $p > 1$, while by eq. (2b), the lipid local concentration rate remains proportional to the template concentration. We shall demonstrate in this section that independent of the value of p, the global dynamics will be exponential in form, although the doubling time or the cycle period will depend on the value of p.

Eqs. (2) implicitly assume that the concentration dilution due to the increase of an individual protocell's volume in the growth–division process is negligible. In other words, the protocell's volume (V_l) can be approximated as a constant and equal to a time-averaged protocell's volume (V_A, a true constant). In the first approximation, the concentrations are calculated with respect to the latter volume (*i.e.* $[X] = N_X/V_A$, where N_X is the number of molecules of type X).

B. Growing-Dividing Protocells

In a second approximation, Rocheleau et al. (2006) consider that the local lipid aggregate volume V_l grows only from the addition of lipid molecules to the aggregate, *i.e.* the contribution of templates, precursors, and fluid to the aggregate volume was neglected. Note that in the case of a micelle, as considered here, both the volume and the surface area (S) of the protocell are proportional to the number of lipids ($V_l \propto S \propto N_L$). That is, as the micelles have no hollow interior, the protocell's volume equals the number of lipids multiplying the volume of a lipid. In this case, the surface equals the number of lipids multiplying πR^2, with R being the radius of a lipid, and thus the surface too is proportional with the number of lipids. In the case of a vesicle, the hollow spherical form introduces a nonlinear dependence between volume and surface ($V_l \propto S^{3/2}; S \propto N_L$) [4].

In the Rocheleau approach, once the dilution effect is taken into account, the concentration of the metabolites must be referred to the time-dependent volume, V_l instead of V_A and thus eq. (2a) must be replaced by

$$\frac{d[T_l]}{dt} = \left.\frac{d[T_l]}{dt}\right|_{V_l} - \left.\frac{[T_l]}{V_l}\frac{dV_l}{dt}\right|_{N_T} = C_T[T_l]^p - \frac{[T_l]}{V_l}\frac{dV_l}{dt}, \quad (3)$$

where the first term on the r.h.s is calculated at constant volume ($V_l = V_A$), while the second, at a constant number of template molecules (see Appendix B). As the lipid aggregates have a characteristic scale, there exists an average number m_0 of lipids per aggregate volume V_A. Theoretically and experimentally, the protocells are expected to grow and become unstable when reaching a critical size, with the instability being resolved by the subsequent division into two daughters.

C. Global Concentrations

In the context of growing-dividing protocells in a tank reactor, the global concentration of metabolites denotes their concentration calculated using the volume of the tank containing the aggregates (l.h.s. of Fig. 1). The global concentration of templates, $[T_g]$ is thus obtained in Rocheleau et al. (2006) as being

$$[T_g] = [T_l][A]V_l \approx [T_l][A]V_A, \quad (4)$$

where $[A]$ is the concentration of aggregates or protocells (number of aggregates per total tank volume), with the local concentration still referring to the intra-aggregate metabolite concentration.

The growth rate of the aggregate concentration, $d[A]/dt$, depends both on the aggregate concentration, $[A]$, and on the growth of the local volume of the aggregates, dV_l/dt. The former is a consequence of the division process, since the greater the number of aggregates that exist, the more will be produced in a finite time interval, while the latter term is an indicator of the doubling time as it illustrates how fast a single aggregate (and implicitly the number of aggregates) grows through the addition of lipids (see also Appendix B):

$$\frac{d[A]}{dt} = [A]\frac{d(N_L/m_0)}{dt} = [A]\frac{1}{V_A}\frac{dV_l}{dt} \quad (5)$$

[3] The value of C_T clearly depends on the value of p. As concentrations have a dimension of $1/V$, V =volume, from eq. (2a), C_T must have dimensions of $1/(V^{p-1}t)$. As K_t has dimensions of $1/V$ and k_T has dimensions of $(1/Vt)$, we note that the definition of C_T following eq. (2a) is correct only for $p = 1/2$ case, but needs to be modified for $p \neq 1/2$.

[4] If all the vesicular protocell's chemistry takes place within the container bilayer itself, then one would still have $V_l \propto S \propto N_L$

Taking the derivative of eq. (4) and using eqs. (4), (5), (B5) and $V_l \approx V_A$, the global dynamics is given by

$$\frac{d[T_g]}{dt} = \gamma_T [T_g] \left(\frac{[T_g]}{[A]}\right)^{p-1} \quad (6)$$

$$\frac{d[A]}{dt} = \gamma_A [T_g], \quad (7)$$

where $\gamma_T \equiv C_T / V_A^{p-1}$ and $\gamma_A \equiv C_L / m_0$. See Appendix B for the detailed derivation of these equations.

Dividing eq. (6) by eq. (7), one finds that

$$\frac{d[T_g]}{d[A]} = \frac{\gamma_T}{\gamma_A} \left(\frac{[T_g]}{[A]}\right)^{p-1}, \quad (8)$$

which when solved leads to:

$$[A] = \begin{cases} \left[\frac{\gamma_A}{\gamma_T}[T_g]^{2-p} + C_0\right]^{\frac{1}{2-p}} & ;\ p \neq 2 \quad (9a) \\ C_1\ [T_g]^{\frac{\gamma_A}{\gamma_T}} & ;\ p = 2 \quad (9b) \end{cases}$$

The constants C_0 and C_1 are defined as $C_0 \equiv [A]_0^{2-p} - \frac{\gamma_A}{\gamma_T}[T_g]_0^{2-p}$ and $C_1 \equiv [A]_0 / [T_g]_0^{\frac{\gamma_A}{\gamma_T}}$, where $[A]_0$ and $[T_g]_0$ denote respectively the aggregate and the template concentrations at $t = 0$. From its definition, $\gamma_A > 0$ and as $[T_g]$ must be positive, thus $d[A]/dt$ is always positive (see eq. [7]). Therefore, the concentration $[A]$ increases in time, independent of the sign of constant C_0. However, the general condition for $C_0 > 0$ is

$$(2-p)\ln\left(V_A \frac{[T_g]_0}{[A]_0}\right) < \ln\,\alpha \quad (10)$$
$$\text{with}\ \ \alpha \equiv \frac{C_T m_0}{C_L V_A}.$$

Eq. (6) can now be rewritten as:

$$\frac{d[T_g]}{dt} = \begin{cases} \gamma_T \left(\frac{\gamma_A}{\gamma_T}\right)^{\frac{1-p}{2-p}} [T_g] \left[1 + \frac{\gamma_T}{\gamma_A}\frac{C_0}{[T_g]^{2-p}}\right]^{\frac{1-p}{2-p}} & ;\ p < 2 \quad (11a) \\ c\ [T_g]^{2-\frac{\gamma_A}{\gamma_T}} & ;\ p = 2 \quad (11b) \\ \gamma_T C_0^{\frac{1-p}{2-p}} [T_g]^p \left[1 + \frac{\gamma_A}{\gamma_T}\frac{1}{C_0 [T_g]^{p-2}}\right]^{\frac{1-p}{2-p}} & ;\ p > 2 \quad (11c) \end{cases}$$

where $c \equiv \gamma_T / C_1$. The complex form of these equations does not allow a direct integration and thus requires the consideration of an approximated solution.

Let us remember that for any exponent β and any real number x satisfying $|x| < 1$, one can use the approximation:

$$(1+x)^\beta = 1 + \beta x + \frac{\beta(\beta-1)}{2!}x^2 + ... \approx 1 + \beta x, \quad (12)$$

with the last approximation being valid for $|x| \ll 1$.

As $[T_g]$ increases with time, one can consider that after a sufficiently long time, the second term in the brackets of eqs. (11a) and (11c) reaches values much smaller than unity and thus the expansion (12) can be applied, leading to

$$\frac{d[T_g]}{dt} \approx \begin{cases} a[T_g] + b[T_g]^{p-1} & ;\ p < 2 \quad (13a) \\ g[T_g]^2 + h[T_g]^p & ;\ p > 2 \quad (13b) \end{cases}$$

where $a \equiv \gamma_T (\gamma_A/\gamma_T)^{\frac{1-p}{2-p}}$, $b \equiv \gamma_T C_0 \frac{1-p}{2-p} \left(\frac{\gamma_A}{\gamma_T}\right)^{\frac{-1}{2-p}}$, $g \equiv \gamma_A C_0^{\frac{-1}{2-p}} \frac{1-p}{2-p}$ and $h \equiv \gamma_T C_0^{\frac{1-p}{2-p}}$. We note that if $C_0 > 0$ for any p, then the constants a, g and h are always positive, with the exception of b which is negative for $p \in (1, 2)$.

Before proceeding, we remark that there is no known real replication process that achieves a growth order $p > 2$. The most efficient replication process known so far involves the hypercycles dynamics and thus $p = 2$. For this reason, we shall concentrate in the following on the cases $p < 2$.

One can recognise eq. (13a) as being a Bernoulli Equation, whose general solution is known and thus the global concentration of templates for $p \leq 2$ is found to be:

$$[T_g]_t = \begin{cases} \dfrac{\{exp[(2-p)at + D_0] - b\}^{\frac{1}{2-p}}}{a^{\frac{1}{2-p}}} & ; p < 2 \quad (14a) \\ (D_1 t + D_2)^{\frac{1}{\gamma_A/\gamma_T - 1}} & ; \ \gamma_A \neq \gamma_T \ ; p = 2 \quad (14b) \\ [T_g]\,(0)\ e^{ct} & ; \ \gamma_A = \gamma_T \ ; p = 2 \quad (14c) \end{cases}$$

where $D_0 = ln[b + a[T_g]_0^{2-p}]$, $D_1 \equiv c(\gamma_A/\gamma_T - 1)$ and $D_2 \equiv [T_g]_0^{\frac{\gamma_A}{\gamma_T}-1}$. It can be seen that the case $p = 1/2$ coincides with eq. 30 from Rocheleau et al. (2006). Also, similar to the reasoning from Rocheleau et al. (2006), for the case $p < 2$, the global template concentration evolves at large times as $[T_g]_t \approx \exp(at)$ [see also their eq. (21)], with the subscript t denoting the time dependence of the global concentrations. Thus, for $p < 2$ and for $p = 2, \gamma_T = \gamma_A$, the functional forms of $[A]_t$ and $[T_g]_t$ after sufficiently long time differ by a constant [eq. (9)], implying that, to a leading order, the coupled template and aggregate growths are both exponential with the same exponent.

More exactly, considering that the constant C_0 becomes neglectable when time and concentration get to be large, the ratio of the templates and aggregates concentration [from eqs. (9a)] behaves as:

$$\frac{[T_g]_t}{[A]_t} \xrightarrow{t\to\infty} \left(\frac{\gamma_T}{\gamma_A}\right)^{\frac{1}{2-p}}, \quad (15)$$

namely the template to aggregate ratio becomes a constant. Next, we remark that as $[T_l] \equiv 2[T_d] + [T_s]$ with $[T_d] \gg [T_s]$, a viable aggregate must have at least one single template or, in a looser version, one double template, otherwise its replication is impossible. Hence, an implicit requirement for a viable system is $[T_g]/[A] \geq 1$ or

$$\gamma_A \leq \gamma_T, \quad (16)$$

for any system characterised by $p < 2$. An example of a simulation that follows eqs. (6) and (7) is given in Fig. 2. We have considered the following values: $m_0 = 1000, k_L = 25\ (\mathrm{Ms})^{-1}, \mathrm{k_T} = 10\ (\mathrm{Ms})^{-1}, [\mathrm{pL}] = 10^{-3}\ \mathrm{M}, \mathrm{V_A} = 5\times10^{-19}$ litres, $\mathrm{K_t V_A} = 1 \times 10^{-3}$ molecules, $f(O) = \alpha[O] = 2 \times 10^{-4}$ M, with $\alpha = 2$ being the number of oligomers necessary in the replication of T_s. The initial conditions are $[T_g]_0 = 10^{-6}$ M and $[A]_0 = 10^{-8}$ M.

However, the case $p = 2, \gamma_T \neq \gamma_A$ does not present coordinated growth, but instead the aggregate concentration grows faster than the template concentration. For this case, using eqs. (9a) and 14b, one obtains

$$\frac{[T_g]_t}{[A]_t} = \frac{1}{C_1}\left[(D_1 t + D_2)^{1/(\gamma_A/\gamma_T - 1)}\right]^{1-\gamma_A/\gamma_T} \quad (17)$$

$$= \frac{1}{C_1(D_1 t + D_2)} \xrightarrow{t\to\infty} 0, \quad (18)$$

confirming a faster growth of the aggregate concentration with respect to the template concentration. The physical interpretation of this result is that, eventually, there will exist many aggregates that contain no templates at all.

Finally, for the case $p > 2$, one notes that at large global template concentrations, eq. (13b) can be approximated further as

$$\frac{d[T_g]}{dt} \approx h[T_g]^p \quad (19)$$

and thus the global template concentration follows the local intra-aggregate growth law, with order p. As such, the global growth law is no longer exponential. Nonetheless, as previously discussed, after a sufficiently long time, eq. (9a) reveals that $[A]_t$ and $[T_g]_t$ differ by a constant. Thus for the cases $p > 2$, the resultant coordinated growth of the population of protocells is characterised by the same exponent as the local intra-aggregate template growth.

Once again, we stress the fact that no known real growth process has an order $p > 2$ and in fact, all theoretical and experimental replication processes present growth orders inferior to the pure hyperbolic case ($p = 2$). We consider as our most important result the derivation that for the real world ($p < 2$), the coupling of the template with the container in a protocellular ensemble results in a coordinated global exponential growth at large times.

V. THREE-ELEMENTS DYNAMICS

A higher level of chemical complexity can be introduced by considering additional reactions for the template replication. This seems a reasonable assumption since experimental template replication requires the activation of the precursors subsequently employed in the replication process. In this sense, we shall consider the introduction of oligomer precursors, pO into the dynamics of the two-elements system presented above. The chemical reactions considered are:

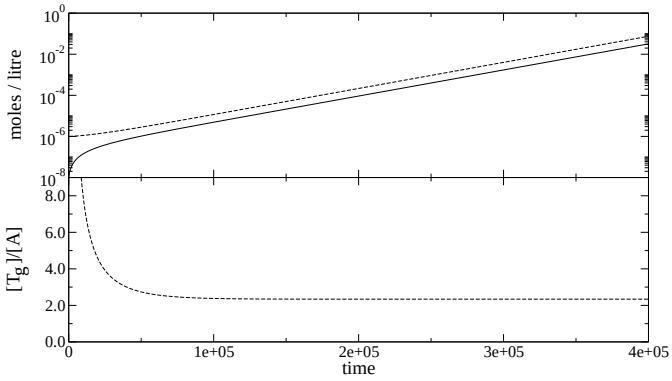

FIG. 2 A simulation of eqs. (6) and (7) for the parabolic case $p = 1/2$: $[A]$ – solid line and $[T_g]$ – dashed line *(upper panel)*; the ratio $[T_g]/[A]$ satisfies eq. (15) *(lower panel)*. See text for details.

$$pO + T_d \xrightarrow{k_O} O + T_d \tag{20a}$$

$$\alpha O + T_s \xrightarrow{k_T} T_d \tag{20b}$$

$$T_d \xleftrightarrow{K_t} 2Ts \tag{20c}$$

$$pL + T_d \xrightarrow{k_L} L + T_d\ , \tag{20d}$$

where the notations from Rocheleau et al. (2006) have been used: T_s – single-stranded template; T_d – double-stranded template; pO and pL – the oligomer and lipid precursors, respectively. A graphical representation of this protocell's chemistry is shown in Fig. 3. The steady state is considered, that is the precursors' concentration is taken as constant. In this case, one can notice that the double-stranded template catalyses both

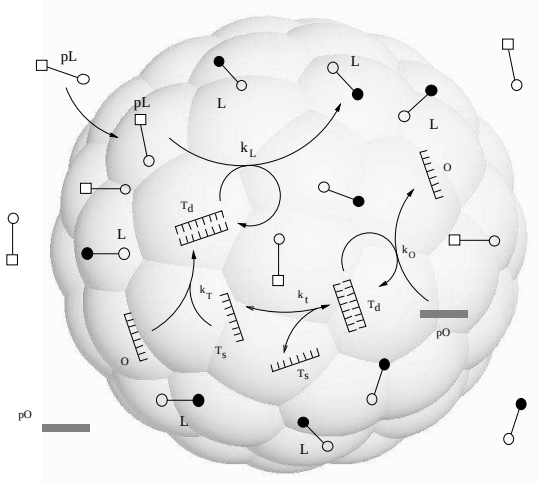

FIG. 3 Protocell reaction network for the three-element scenario. In this case, the container is coupled to the template through an additional reaction structure where precursors of templates need to be transformed, the transformation being catalysed by templates.

lipid and oligomer formation. As in the previous section, we use the total local template concentration $[T_l] \equiv 2[T_d] + [T_s] \approx 2[T_d]$ as the template variable and take into account the effect of volume change with time. Considering the kinetics of this system, the concentration of templates and oligomers can be respectively written as

$$[\dot{T}_l] = \alpha k_T [O_l] \sqrt{\frac{K_t [T_l]}{2}} - \frac{d[A]}{dt}\frac{[T_l]}{[A]} \tag{21a}$$

$$[\dot{O}_l] = k_O [pO]\frac{[T_l]}{2} - k_T [O_l]\sqrt{\frac{K_t [T_l]}{2}} - \frac{d[A]}{dt}\frac{[O_l]}{[A]} \tag{21b}$$

As in the previous section, the transition from local to global is based on the expressions $[T_g] = [T_l]\ [A]\ V_A$ and $[O_g] = [O_l]\ [A]\ V_A$. Thus the final system of coupled equations is:

$$[\dot{T}_g] = \gamma_T\ [O_g] \sqrt{\frac{[T_g]}{[A]}} \tag{22a}$$

$$[\dot{O}_g] = \gamma_O\ [T_g] - \gamma_T\ [O_g] \sqrt{\frac{[T_g]}{[A]}} \tag{22b}$$

$$[\dot{A}] = \gamma_A\ [T_g], \tag{22c}$$

with

$$\gamma_O \equiv \frac{k_O\ [pO]}{2};\ \ \gamma_T \equiv \alpha k_T \sqrt{\frac{K_t}{2V_A}};\ \ \gamma_A \equiv \frac{k_L\ [pL]}{2m_0}\ , \tag{23}$$

where m_0 is again the average number of lipid molecules per aggregate and $K_t = [T_s]^2/[T_d]$ resulting from the equilibrium condition of reaction 20c. Fig. 4 illustrates an example of a solution of eqs. (22). The behaviour appears to be representative of the generic dynamics of the entire range of parameters investigated. Below, we shall demonstrate that this case is also characterised by coordinated exponential growth after a sufficiently long time, with the same exponent for the oligomer, template and aggregate concentration.

A. Linear stability analysis

The nonlinear system from eqs. (22) has $([O_g], [T_g], [A]) = ([O_g]_0, 0, [A]_0)$ as a unique fixed point that results to be unstable under perturbation, implying that these variables tend to infinity when time tends to infinity. In other words, a protocell whose chemistry is given by eqs. (20), but containing no template molecules, will not grow. On the contrary, a protocell containing template molecules will grow and replicate, producing the increase in the global metabolites' concentrations. Employing a change of variables, we shall prove below that the global variables follow an exponential growth.

As we start with at least one aggregate and protocells' death is not contemplated, we conclude that the following variables can be well defined: $x \equiv [T_g]/[A]$ and $y \equiv [O_g]/[A]$. Using these variables, eqs. (22) reduce to:

$$\frac{dx}{dt} = \frac{[\dot{T_g}][A] - [T_g][\dot{A}]}{[A]^2} = \gamma_T y x^{1/2} - \gamma_A x^2 \quad (24a)$$

$$\frac{dy}{dt} = \frac{[\dot{O_g}][A] - [O_g][\dot{A}]}{[A]^2} = \gamma_O x - \gamma_T y x^{1/2} - \gamma_A x y \quad (24b)$$

We are interested in studying the dynamics of eqs. (24) in order to infer the long-term behaviour of eqs. (20). In particular, we are interested in whether the ratios x and y stabilise. For this purpose, we note that the former system has two fixed points resulting from the conditions $\dot{x} = 0$ and $\dot{y} = 0$: the trivial one, $(x_1, y_1) = (0, y_0)$ and a second one, (x_2, y_2) which is the solution of the equations:

$$\gamma_T \; y - \gamma_A \; x^{3/2} = 0; \quad \gamma_O - \gamma_A \; x - \frac{\gamma_A^2 \; x^{3/2}}{\gamma_T} = 0 \quad (25)$$

The trivial fixed point illustrates the fact that no evolution is possible in the absence of templates. Thus, we are only interested in the nontrivial case when the initial template concentration is non-zero, that is we shall concentrate on the characteristics of the fixed point (x_2, y_2). In order to determine its stability, the Jacobi matrix has to be calculated and evaluated at the fixed point:

$$J_2 \equiv \begin{pmatrix} \frac{\partial \dot{x}}{\partial x} & \frac{\partial \dot{x}}{\partial y} \\ \frac{\partial \dot{y}}{\partial x} & \frac{\partial \dot{y}}{\partial y} \end{pmatrix}_{(x_2, y_2)} = \begin{pmatrix} -\frac{3}{2}\gamma_A x_2 & \gamma_T x_2^{1/2} \\ \frac{1}{2}\gamma_A x_2 & -\gamma_T x_2^{1/2} - \gamma_A x_2 \end{pmatrix}$$

where eq. (25) has been employed to simplify the Jacobi matrix, that is we used $y_2 = x_2^{3/2}\gamma_A/\gamma_T$. The eigenvalues λ, which provide the stability information of (x_2, y_2), result from the characteristic equation $\det(J_2 - \lambda I) = 0$, where I is the identity matrix:

$$\lambda^2 + a\lambda + b = 0 \quad (26)$$

$$a \equiv \gamma_T x_2^{1/2} + \tfrac{5}{2}\gamma_A x_2; \quad b \equiv \gamma_T \gamma_A x_2^{3/2} + \tfrac{3}{2}\gamma_A^2 x_2^2 \quad (27)$$

$$\Delta \equiv a^2 - 4b = \gamma_T^2 x_2 + \tfrac{\gamma_A^2 x_2^2}{4} + \gamma_T \gamma_A x_2^{3/2} > 0 \quad (28)$$

It can be seen that since $a, b > 0$ and $\Delta > 0$, the eigenvalues are real and negative (Routh-Hurwitz criterion), leading to the conclusion that the fixed point (x_2, y_2) is stable, and implicitly that (x_1, y_1) is unstable.

Returning to eqs. (22) and to the definition of x and y, one can now see that after a sufficiently long time, the following approximations hold:

$$\frac{[T_g]}{[A]} \xrightarrow{t\to\infty} x_2 \quad (29a)$$

$$\frac{[O_g]}{[A]} \xrightarrow{t\to\infty} y_2 \; , \quad (29b)$$

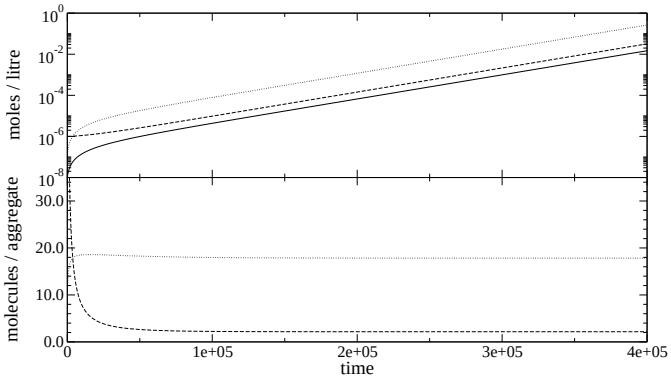

FIG. 4 A simulation of eq. (22) with $k_O = 5$ $(\mathrm{Ms})^{-1}$, $k_T = 15$ $(\mathrm{Ms})^{-1}$ and the rest of parameters having the values employed in Fig. 2. The values of the final constants are $\gamma_O = 2.5 \times 10^{-4}$, $\gamma_T = 2.2 \times 10^{-6}$ and $\gamma_A = 1.25 \times 10^{-5}$. $[A]$ – solid line, $[T_g]$ – dashed line and $[O_g]$ – dotted line *(upper panel)*; the ratio $[T_g]/[A]$ – dashed line and $[O_g]/[A]$ – dotted line.

which translate into $[\dot{A}] \approx \gamma_A x_2 [A]$ with the use of eq. (22c), and thus into an exponential increase of the aggregate concentration. Since $[A]$ grows exponentially, and after a sufficiently long time, $[T_g]$, $[O_g]$ and $[A]$ differ by a constant, all the variables grow exponentially with the same exponent. We emphasise once more that this behaviour is satisfied only after a sufficiently long time.

Additionally, one can employ eqs. (25) to show that the second fixed point satisfies the relation: $x_2 + y_2 = \gamma_0/\gamma_A$ (Fig. 4).

VI. FOUR-ELEMENTS DYNAMICS

Here we consider a more complete and realistic protocellular system incorporating and explicit metabolism driven by a light-activated sensitiser molecule (Rasmussen et al. 2003). The set of reactions is:

$$Z + pO + T_d \xrightarrow{k_\mathrm{O}} O + T_d + Z \quad (30a)$$

$$\alpha O + T_s \xrightarrow{k_\mathrm{T}} T_d \quad (30b)$$

$$T_d \xleftrightarrow{K_t} 2Ts \quad (30c)$$

$$Z + pL + T_d \xrightarrow{k_\mathrm{L}} T_d + L + Z \quad (30d)$$

$$Z + pZ + T_d \xrightarrow{k_\mathrm{Z}} 2Z + T_d \; , \quad (30e)$$

where the added components are the sensitiser and its precursor, Z and pZ, respectively. The sensitiser absorbs light energy to drive the conversion of the precursor molecules to their products. See Fig. 5.

Again, the standard kinetic differential equations associated with the global variables of this chemical network are easily recovered:

$$\frac{d[T_g]}{dt} = \gamma_T[O_g]\sqrt{\frac{[T_g]}{[A]}} \tag{31a}$$

$$\frac{d[O_g]}{dt} = \gamma_O[Z_g]\frac{[T_g]}{[A]} - \gamma_T[O_g]\sqrt{\frac{[T_g]}{[A]}} \tag{31b}$$

$$\frac{d[Z_g]}{dt} = \gamma_Z[Z_g]\frac{[T_g]}{[A]} \tag{31c}$$

$$\frac{d[A]}{dt} = \gamma_A[Z_g]\frac{[T_g]}{[A]}, \tag{31d}$$

where the constants are defined as:

$$\gamma_O \equiv \frac{k_O[pO]}{2V_A} \; ; \; \gamma_T \equiv \alpha k_T\sqrt{\frac{K_t}{2V_A}}$$
$$\gamma_Z \equiv \frac{k_Z[pZ]}{2V_A} \; ; \; \gamma_A \equiv \frac{k_L[pL]}{2m_0V_A}$$

The system from eqs. (31) can be simplified through the change of variable: $x \equiv [T_g]/[A], y \equiv [O_g]/[A], z \equiv [Z_g]/[A]$, variables that are well defined as $[A] \neq 0$ following the reasoning employed in the previous section. With this change of variables, the system becomes:

$$\frac{dx}{dt} = \gamma_T y\sqrt{x} - \gamma_A x^2 z \tag{32a}$$

$$\frac{dy}{dt} = \gamma_0 xz - \gamma_T y\sqrt{x} - \gamma_A xyz \tag{32b}$$

$$\frac{dz}{dt} = \gamma_Z xz - \gamma_A xz^2. \tag{32c}$$

Similar to the study of the three-elements system, we are interested again in the nontrivial fixed point of eqs. (32), considering that the variables x, y and z can take only positive values. The trivial dynamics (no growth) is characterised by $x_0 = 0$ and/or $z_0 = 0$. The non trivial fixed point of eqs. (32) results from $\dot{x} = \dot{y} = \dot{z} = 0$ with $x \neq 0$ and $z \neq 0$ and it is:

$$(x_2, y_2, z_2) = (\tilde{x}, \frac{\gamma_Z}{\gamma_T}\tilde{x}\sqrt{\tilde{x}}, \frac{\gamma_Z}{\gamma_A}) \tag{33}$$

$$\text{with} \qquad \tilde{x}\sqrt{\tilde{x}} + \frac{\gamma_T}{\gamma_Z}\tilde{x} - \frac{\gamma_O\gamma_T}{\gamma_A\gamma_Z} = 0, \tag{34}$$

with the subscript 0 denoting again the initial conditions, while $\tilde{x}$ is the only positive root of eq. (34), a conclusion drawn from applying the Routh-Hurwitz criterion to this third order equation in $\sqrt{x}$. We are not interested in the exact form of $\tilde{x}$, but rather in pointing out its existence and uniqueness in the positive-values domain, both features resulting from the Routh-Hurwitz criterion. Through eq. (31c), this existence leads to $[\dot{Z}_g] \xrightarrow{t\to\infty} \gamma_Z\tilde{x}[Z_g]$, implying an exponential growth of the sensitiser concentration after a sufficiently long time. This result allows us to conclude, with the use of eq. (33), that the temporal evolution of all metabolites' concentration is exponential, of the type $\propto \exp(at)$, with $a = \gamma_Z\tilde{x}$.

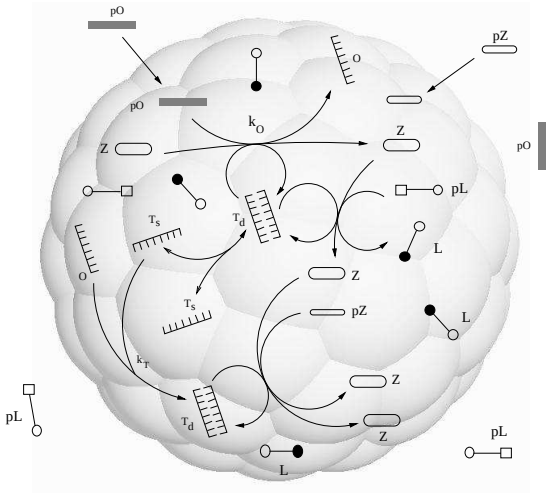

FIG. 5 A full protocell model with an explicit metabolism, container, and informational molecules. All transformations are coupled through template replication. The molecule Z indicates a sensitiser which is able to take energy from an external (not indicated) source of energy (e.g. light).

VII. DISCUSSION

There is ongoing debate in the scientific community on the issue of stoichiometric versus catalytic coupling as a necessary dynamics to ensure balanced parallel growth and correct replication of the constituent systems of such a protocell: metabolism, genome and membrane. In the past 20 years, significant experimental efforts have been dedicated to the optimisation of self-replicating molecules in order to achieve efficient copying (Paul & Joyce 2004). More precisely, several chemical subsystems must be optimised in order to provide an overall self-replicating system that exhibits efficient auto-catalytic behaviour. The efficiency is directly reflected in the degree of catalysis or the order of reaction, where a value of 1 (exponential growth, recall Table I) is believed to provide the appropriate basis of Darwinian selection: survival of the fittest (Szathmáry & Maynard-Smith 1997).

From the modelling point of view, Gánti's chemoton model (Gánti 1975) is a protocell model incorporating all three necessary subsystems in a very tightly coupled and synchronised interdependence (THIS ISSUE Mavelli & Ruiz-Miranzo 2006). This model is the basic example of cyclic stoichimetric coupling as the main coordinating factor. In the present work, we extend a catalytically coupled protocell model (Rocheleau et al. 2006) and demonstrate that the catalytic coupling of the subsystems is sufficient to lead the whole system into balanced exponential growth. In other words, the metabolism-template-container feedback by itself ensures an overall exponential growth of the system in spite of subexponential or supraexponential local growth of its component subsystems. We believe that this result may have implications

for prebiotic and origin of life scenarios, as it is a robust means of providing exponential growth of protocells and thus early Darwinian selection.

In tight connection with the present work, we mention the work of (Serra et al. 2006 (In press). It is also inspired by the Los Alamos Bug and the results of the detailed analytic study therein totally support the coordinated growth of a general class of catalytically coupled protocellular systems.

Acknowledgments

This work is supported in part by the Los Alamos National Laboratory LDRD-DR grant on "Protocell Assembly" (PAs), by the European Commission's 6th Framework project on "Programmable Artificial Cell Evolution" (PACE) and by FIS2004-05422. We thank Gil Benko, Jerzy Maselko and CSL, PACE and PAs colleagues for useful discussions.

References

Bachman, P. A., Luisi, P. L. & Lang, J. 1992, Autocatalytic self-replicating micelles as models for prebiotic structures, *Nature* **357**, 57–59.

Bag, B. G. & von Kiedrowski, G. 1996, Templates, autocatalysis and molecular replication, *Pure & Appl. Chem.* **68**, 2145–2152.

Eigen, M. 1971, Self-oragization of matter and the evolution of biological macromolecules, *Naturwiss.* **58**, 465–526.

Eigen, M. & Schuster, P. 1979, *The Hypercycle: A Principle of Natural Self-Organization*, Berlin: Springer.

Gánti, T. 1975, Organization of chemical reactions into dividing and metabolizing units: the chemotons, *Biosystems* **7**, 189–195.

Gánti, T. 2003, *The principles of life*, Oxford University Press.

Kaneko, K. & Yomo, T. 2000, Symbiotic speciation from a single genotype, *Proc. R. Soc. Lond. B* **267**, 2367–2373.

Lee, D. H., Granja, J. R., Martinez, J. A., Severin, K. & Ghadiri, M. R. 1996, A self-replicating peptide, *Nature* **382**, 525–528.

Luisi, P. L., Ferri, F. & Stano, P. 2006, Approaches to semi-synthetic minimal cells: a review, *Naturwissenschaften.* **93**, 1–13.

Mavelli, F. 2004, *Theoretical investigations on autopoietic replication mechanisms*, PhD thesis, Eidgenössische Technische Hochschule ETH Zürich.

Mavelli, F. & Ruiz-Miranzo, K. 2006, Stochastic simulations of minimal self-reproducing cellular systems, *Phil. Trans. R. Soc. B.* **THIS ISSUE**.

Monnard, P., Apel, C. L., Kanavarioti, A. & Deamer, D. 2002, Influence of ionic solutes on self-assembly and polymerization processes related to early forms of life: Implications for a prebiotic aqueous medium, *Astrobiology* **2**, 213–219.

Oparin, A. I. 1957, *The origin of life on earth*, Oliver and Boyd, London.

Orgel, L. E. 1992, Molecular replication, *Nature* **358**, 203–209.

Paul, N. & Joyce, G. F. 2004, Minimal self-replicating systems, *Curr. Opinion Chem. Biol.* **8**, 634–9.

Rasmussen, S., Chen, L., Deamer, D., Krakauer, D. C., Packard, N. H., Stadler, P. F. & Bedau, M. A. 2004, Transition from Nonliving to Living Matter, *Science* **303**, 963–965.

Rasmussen, S., Chen, L., Nilsson, M. & Abe, S. 2003, Bridging nonliving and living matter, *Artificial Life* **9**, 269–316.

Robertson, A., Sinclair, A. J. & Philp, D. 2000, Minimal self-replicating systems, *Chem. Soc. Rev.* **29**, 141–152.

Rocheleau, T., Rasmussen, S., Nielsen, P. E., Jacobi, M. N. & Ziock, H. 2006, Emergence of protocellular growth laws, *Phil. Trans. R. Soc. B.* **This issue**.

Segré, D., Ben-Eli, D., Deamer, D. & lancet, D. 2001, The Lipid World, *Orig. Life Evol. Biosph.* **31**, 119–145.

Serra, R., Carletti, T. & Poli, I. 2006 (In press), Synchronization phenomena in surface-reaction models of protocells, *Artificial Life* .

Stadler, B. & Stadler, P. 2003, Molecular replicator dynamics, *Adv. Comp. Syst.* **6**, 47–77.

Szathmáry, E. 1991, Simple Growth laws and Selection Consequences, *Trends Ecol. Evol.* **6**, 366–370.

Szathmáry, E. & Maynard-Smith, J. 1997, From Replicators to Reproducers: the First Major Transitions Leading to Life, *J. Theor. Biol.* **187**, 555–571.

Szostak, J. W., Bartel, D. P. & Luisi, P. L. 2001, Synthesizing life, *Nature* **409**, 387–390.

Takakura, K., Toyota, T. & Sugawara, T. 2003, A Novel System of Self-Reproducing Giant Vesicles, *J. Am. Chem. Soc.* **125**, 8134–8140.

von Kiedrowski, G. 1986, A self-replicating hexadeoxynucleotide, *Angew. Chem. Int. Edn. Engl.* **25**, 932.

von Kiedrowski, G., Wlotzka, B., Helbing, J., Matzen, M. & Jordan, S. 1991, Parabolic growth of a hexadeoxynucleotide with a 3'-5'-phos-phor-amidate linkage, *Angew. Chem. Int. Edn. Engl.* **30**, 423–426.

APPENDIX A

The derivation of eqs. (2) is detailed in Rocheleau et al. (2006) and described in brief below. The standard chemical kinetics applied to the reactions (1) yields the following differential equations characterising the temporal evolution of the metabolites' concentration:

$$[\dot{T}_s] = 2K_t[T_d] - k_T[pO][T_s] \quad \text{(A1a)}$$

$$[\dot{T}_d] = -K_T[T_d] + k_T[pO][T_s] \quad \text{(A1b)}$$

$$[\dot{L}] = k_L[pL][T_d], \quad \text{(A1c)}$$

where the chemical equilibrium of reaction (1b) has been used through its equilibrium constant K_t. Considering that the total concentration of (single-)template can be written as $[T_l] \equiv 2[T_d] + [T_s]$, one can rewrite eqs. (A1) in terms of $[T_l]$ as

$$[\dot{T}_l] = k_T[pO][T_s] \quad \text{(A2a)}$$

$$[\dot{L}] = k_L[pL][T_d]. \quad \text{(A2b)}$$

In addition, as the equilibrium constant satisfies $K_t = [T_s]^2/[T_d]$, the following equation holds:

$$2[T_s]^2 + K_t[T_s] - K_t[T_l] = 0,$$

implying that

$$\begin{aligned}[T_s] &= \frac{-K_t + \sqrt{K_t^2 + 8K_t[T_l]}}{4} \approx \frac{\sqrt{K_t[T_l]}2}{} \\ [T_d] &= \frac{[T_l]}{2} + \frac{-K_t + \sqrt{K_t^2 + 8K_t[T_l]}}{4} \approx \frac{[T_l]}{2},\end{aligned}$$

where the product inhibition has been taken into account as $[T_s] \ll [T_d]$. With the help of these approximations, eqs. (A2) can finally be rewritten as eqs. (2).

APPENDIX B

Eqs. (2) implicitly assume that the protocell's volume can be approximated as being a constant. Thus one can also write eq. (2b) as

$$\frac{1}{V_A}\frac{dN_L}{dt} = C_L[T_l]. \tag{B1}$$

If instead, the volume V_l is considered proportional to the number of lipid molecules, *i.e.*, $V_l = Q \times N_L$, with Q being the proportionality constant, then the volume must be considered as time-varying:

$$\frac{dV_l}{dt} = Q \times \frac{dN_L}{dt} \tag{B2}$$

Thus, in the changing volume approach, the time derivative of the template concentration $[T_l] \equiv N_T/V_l$ is given by:

$$\frac{d[T_l]}{dt} = \frac{1}{V_l}\frac{dN_T}{dt}\bigg|_{V_l} - \frac{N_T}{V_l^2}\frac{dV_l}{dt}\bigg|_{N_T} \tag{B3}$$

The first term on the r.h.s of eq. (B3) is considered at constant volume and thus one must have:

$$\frac{d[T_l]}{dt}\bigg|_{V_l} = \frac{1}{V_l}\frac{dN_T}{dt}\bigg|_{V_l} \tag{B4}$$

By using the definition of $[T_l]$ and eqs. (B4) and (2a), both of which apply at constant volume, eq. (B3) can be rewritten as

$$\frac{d[T_l]}{dt} = C_T[T_l]^p - \frac{[T_l]}{V_l}\frac{dV_l}{dt} \tag{B5}$$

Next, we consider the dividing protocells and their concentration, $[A]$ in the entire experimental volume. As the lipid aggregates have a characteristic scale, there exists and average number m_0 of lipids per average aggregate volume V_A. Thus, the growth rate of $[A]$ is given by:

$$\begin{aligned}\frac{d[A]}{dt} &= [A]\frac{d}{dt}(N_L/m_0) \\ &= \frac{[A]}{m_0}\frac{dN_L}{dt} \\ &= \frac{[A]}{Qm_0}\frac{dV_l}{dt} \qquad \text{(B6)} \\ &= \frac{C_L}{m_0}[T_g] \qquad \text{(B7)}\end{aligned}$$

where $[T_g] = [A]V_a[T_l]$ and eq. (B1) have been used. One can recognise eq. (B7) as being eq. (7) with $\gamma_A \equiv C_L/m_0$. Applying eq. (B2), one can rewrite eq. (B6) as

$$\begin{aligned}\frac{dA}{dt} &= \frac{[A]}{Qm_0}\frac{dV_l}{dt} \\ &= \frac{[A]}{V_A}\frac{dV_l}{dt} \qquad \text{(B8)}\end{aligned}$$

where we have used the definition of the average aggregate volume ($V_A = Qm_0$). One can recognise the last equation as being eq. (5).

Finally, let us recover the evolution of the global concentration of templates. Taking the derivative of $[T_g] = [A]V_A[T_l]$ yields

$$\frac{d[T_g]}{dt} = [T_l]V_A\frac{d[A]}{dt}\bigg|_{[T_l]} + [A]V_A\frac{d[T_l]}{dt}\bigg|_{[A]} \tag{B9}$$

Using eqs. (B8) and (B5) to substitute into the first and second terms on the r.h.s of eq. (B9), we have

$$\begin{aligned}\frac{d[T_g]}{dt} &= [T_l]\frac{[A]}{Qm_0}\frac{dV_l}{dt} + [A]V_A\left(C_T[T_l]^p - \frac{[T_l]}{V_l}\frac{dV_l}{dt}\right) \\ &= [A]V_AC_T[T_l]^p - [A][T_l]\frac{dV_l}{dt}\left[\frac{1}{V_l} - \frac{1}{Qm_0}\right] \qquad \text{(B10)}\end{aligned}$$

Considering again the approximation $V_l \approx V_A$, the bracketed r.h.s of eq. (B10) becomes zero. Then using the relation between $[T_g]$ and $[T_l]$, one obtains

$$\frac{d[T_g]}{dt} = C_T[T_g]\left(\frac{[T_g]}{V_A[A]}\right)^{p-1} = \gamma_T[T_g]\left(\frac{[T_g]}{[A]}\right)^{p-1}$$

with $\gamma_T \equiv C_T/V_A^{p-1}$, which is eq. (6).